ER stress disturbs SR/ER-mitochondria Ca2+transfer: Implications in Duchenne muscular dystrophy

Marion Pauly, Claire Angebault, Haikel Dridi, Cécile Notarnicola, Valérie Scheuermann, Alain Lacampagne, Stefan Matecki, J. Fauconnier

ER stress disturbs SR/ER-mitochondria Ca^{2+} transfer: Implications in Duchenne muscular dystrophy

Marion Pauly[a,b], Claire Angebault-Prouteau[b,1], Haikel Dridi[b,1], Cécile Notarnicola[b], Valérie Scheuermann[b], Alain Lacampagne[b], Stefan Matecki[b], Jérémy Fauconnier[b,*]

[a] Inserm U1055, Hypoxie et Physiopathologies, Université Grenoble Alpes, Grenoble, France
[b] Inserm U1046, UMR CNRS 9214, Université Montpellier, CHRU Montpellier, Montpellier, France

Keywords:
mdx
Diaphragm
UPR
Calcium signaling

A B S T R A C T

Besides its role in calcium (Ca^{2+}) homeostasis, the sarco-endoplamic reticulum (SR/ER) controls protein folding and is tethered to mitochondria. Under pathophysiological conditions the unfolded protein response (UPR) is associated with disturbance in SR/ER-mitochondria crosstalk. Here, we investigated whether ER stress altered SR/ER-mitochondria links, Ca^{2+} handling and muscle damage in WT (Wild Type) and *mdx* mice, the murine model of Duchenne Muscular Dystrophy (DMD). In WT mice, the SR/ER-mitochondria links were decreased in isolated FDB muscle fibers after injection of ER stress activator tunicamycin (TM). Ca^{2+} imaging revealed an increase of cytosolic Ca^{2+} transient and a decrease of mitochondrial Ca^{2+} uptake. The force generating capacity of muscle dropped after TM. This impaired contractile function was accompanied by an increase in autophagy markers and calpain-1 activation. Conversely, ER stress inhibitors restored SR/ER-mitochondria links, mitochondrial Ca^{2+} uptake and improved diaphragm contractility in *mdx* mice. Our findings demonstrated that ER stress-altered SR/ER-mitochondria links, disturbed Ca^{2+} handling and muscle function in WT and *mdx* mice. Thus, ER stress may open up a prospect of new therapeutic targets in DMD.

1. Introduction

A tight control of calcium (Ca^{2+}) homeostasis is essential for normal function and the survival of skeletal muscle. The sarco-endoplasmic reticulum (SR/ER) constitutes an extensive network within the muscle fiber playing a central role in Ca^{2+} homeostasis as well as in protein synthesis, folding, sorting and quality control. Although these functions are performed in different area of the SR/ER [1], they are closely linked and altered SR/ER Ca^{2+} homeostasis may impact protein folding [2]. Indeed, to limit accumulation of unfolded and misfolded proteins, the stressed ER triggers an homeostatic response called Unfolded Protein Response (UPR) [3]. This signaling pathway involves three transmembrane receptors, the pancreatic ER kinase (PKR)-like ER kinase (PERK), the activating transcription factor 6 (ATF6) and the inositol-requiring enzyme 1 (IRE1α). Under basal conditions, they are inactivated by the chaperone-binding protein/glucose regulated protein 78 (Bip/ GRP78) [4]. Under ER stress, GRP78 dissociates from ER membranes proteins and migrates in the ER lumen to bind unfolded and misfolded proteins. Consequently, IRE1α, PERK and ATF6 signaling pathways are activated to limit proteins translation, increase unfolding proteins degradation and promote chaperone expression involved in proteins folding. If the adaptive UPR response fails to restore proteins homeostasis in the ER lumen, cellular signaling switches from pro-survival to pro-death with apoptosis activation [5].

Mitochondria and SR/ER are physically interconnected organelles with contact points delimitating an exchange space referred to as mitochondria-associated ER membranes (MAMs). Within MAMs, the voltage-dependent anionic channel (VDAC) located on the mitochondrial outer membrane is physically and functionnaly linked to the inositol-1,4,5-triphosphate receptor (IP3R), on the ER membrane, *via* the chaperone GRP75 [6]. This complex allows a direct Ca^{2+} transfer from the ER to mitochondria [7] and is crucial for cell fate, energy metabolism

Abbreviations: ATF6, activating transcription factor 6; ATP, Adenosine triphosphate; CTL, Control; Ddit3, DNA damage inducible transcript 3; DMD, Duchenne Muscular Dystrophy; EDL, Extensor Digitorum Longus; EIF2α, eukaryotic translation initiation factor 2A; FBS, fetal bovine seum; FDB, Flexor Digitorum Brevis; GRP75, glucose regulated protein 75; GRP78, glucose regulated protein 78; IP3R, inositol 1,4,5-triphosphate receptor; IRE1α, inositol-requiring enzyme 1; LC3, microtubule-associated protein 1 light chain 3 alpha; PERK, protein kinase R (PKR)-like ER kinase; RPLP0, ribosomal protein large P0; RPS14, Ribosomal protein S14; TM, Tunicamycin; TUDCA, tauro-ursodeoxycholic acid; ULK1, Unc-51 like autophagy activating kinase 1; UPR, Unfolded Protein Response; VDAC, voltage-dependent anion channel

* Corresponding author at: UMR CNRS 9214-Inserm 1046, CHU Arnaud De Villeneuve, Bât Crastes de Paulet, 371 Avenue du Doyen Gaston Giraud, 34295 Montpellier cedex, France.
E-mail address: jeremy.fauconnier@inserm.fr (J. Fauconnier).

[1] Both authors contribute equally to this work.

and Ca^{2+} homeostasis. A disruption of ER-mitochondria contact points disturbs Ca^{2+} transfer and may promote ER stress [8].

Increased UPR has been demonstrated in several myopathy such as spinal bulbar muscular atrophy [9], myotonic dystrophy type I [10], autoimmune myositis [11] or tibial muscular dystrophy [12]. More recently, in Duchenne muscular dystrophy (DMD) patients, increased ER stress has also been reported [13]. DMD, a X-linked disorder, results from dystrophin deficiency due to nonsense mutations [14]. In the absence of dystrophin, muscular contraction is impaired [15] with an altered Ca^{2+} handling [16–22], a mitochondrial dysfunction [23–25], an oxidative stress [26] and cell death [27,28]. Although the disturbed striated muscle function in DMD is well established, whether ER stress contributes to the setting of the pathology remains to be elusive.

In the present study, we thus aimed to determine whether ER stress alters muscle function in WT as well as in *mdx* mice, a mouse model of DMD. After a pharmacological induction of ER stress in WT mice, with the N-glycosylation inhibitor tunicamycin (TM), we demonstrated a disruption in SR/ER-mitochondria interaction and Ca^{2+} transfer associated with an impaired muscle function. Conversely, in *mdx* mice, ER stress inhibition with TUDCA improved SR/ER-mitochondria interaction and muscle contractility. This study provides, for the first time, functionnal evidences of impaired SR/ER-mitochondria interaction under ER stress in DMD.

2. Materials and methods

2.1. Animals

The study was approved by the institutional ethics committee for animal experiments, Languedoc Roussillon (no CEEA-LR-12078). Different ages (4, 10 and 26 weeks old male) of *mdx* or WT (Wild-Type, C57BL6) mice (Janvier SAS, Le Genest Saint Isle, France) were used in this study. To induce an ER stress, 10 weeks old WT mice received a single intraperitoneal injection of tunicamycin (a N-glycosylation inhibitor) at 1 mg/kg body weight [29]. Untreated littermate mice were injected in the same manner with vehicle (0.9% NaCl). *In vivo,* TM is toxic and provokes premature death within the first 24 h. We therefore limited TM exposure as short as possible. Thus, mice were sacrificed after 8 h of injection as previously described [30,31] and diaphragm muscles were dissected and stored. FDB muscles were used for isolated single muscle fiber experiments. Diaphragms were flash frozen in liquid nitrogen for immunoblotting and gene expression analysis. In order to inhibit ER stress, *mdx* mice received intraperitoneal injection of TUDCA (Calbiochem) at a daily dose of 500 mg/kg body weight (5 consecutive days per week) for four weeks.

2.2. Preparation and culture of muscle fibers

Single muscle fibers were enzymatically isolated from FDB following a protocol derived from that described by Head [32]. After dissection FDB muscles were placed in a petri dish filled with DMEM (GIBCO-31966) containing 0.1% streptomycin/penicilin (Gibco-0906) 10% fetal bovine serum (FBS) and 0,3% type Ia collagenase (C9891 type Ia, Sigma-Aldrich, Milano, Italy) for 45 min at 37 °C in a water-saturated incubator with 5% CO2. After three washes in Tyrode solution (mM: NaCl 140, KCl 2, $CaCl_2$ 2, Hepes 10, and glucose 5) containing 10% FBS to block the collagenase effect and stabilize the fibers, the muscles were gently and repeatedly sucked in and out a fire-polished Pasteur pipettes of different diameters (30–300 µm) inside a glass Falcon until muscle fibers were dissociated. Dissociated fibers were placed in petri dish with a bottom glass covered with mouse laminin. Culture dishes were kept in incubator at 37 °C, 5% CO_2.

2.3. Ca^{2+} measurements

Ca^{2+} time course was evaluated using confocal imaging in a native cell environment in the presence of extracellular calcium (1.8 mM $CaCl_2$) [33]. To measure cytosolic Ca^{2+}, cells were loaded with fluo-4 AM (5 µM, Molecular Probes, Eugene, OR), 20 min at room temperature. After being loaded, cells were placed on the stage of a Zeiss LSM 510 inverted confocal microscope (Zeiss, Le Pecq France) equipped with a 25 × lens (H_2O immersion, Numerical Aperture, NA = 1.2). An excitation wavelength of 488 nm was used, and emitted light was collected through a 505 nm long-pass filter. The laser intensity used (3%–6% of the maximum) had no noticeable deleterious effect on the fluorescence signal or cell function over the course of the experiment. Rhod-2 AM was used to measure mitochondrial Ca^{2+} variations. Muscle cells were loaded with rhod-2 AM (3 µM) for 30 min at 37 °C followed by washout and kept at least 1 h at room temperature, prior experiments, to optimize mitochondrial loading. Rhod-2 fluorescence signals were obtained by excitation at 568 nm and measuring the emitted light at 585 nm. In a set of experiments, we analyzed mitochondrial Ca^{2+} uptake after a single 100 Hz or 300 Hz tetanus as described previously [34–36]. Briefly, loaded fibers were line-scanned along the long axis of the fiber and the rhod-2 signal was calculated by subtracting the anisotropic band (F_A = non-mitochondrial signal) to the isotropic band (F_I = mitochondrial signal) before and 1 s after the stimulation. Mitochondrial Ca^{2+} uptake was expressed as F/F_0, where F_0 is the rhod-2 signal (F_I–F_A) before the stimulation and F the rhod-2 signal (F_I–F_A) after the stimulation (Fig. 2D). Collected images were processed with ImageJ (NIH, USA; http://rsb.info.nih.gov/ij/).

2.4. In situ proximity ligation assay

In situ proximity ligation assay (PLA) was used to detect *in situ* protein-protein interactions within a 40 nm range with high specificity and sensitivity as previously described [37]. Briefly, after dissociation, fibers were fixed and permeabilized and *in situ* PLA analysis were performed according to the manufacturer's protocol (OLINK Bioscience). Fibers were incubated with the primary antibodies overnight at 4 °C and then washed three times with PBS-0.1% Tween 20. The following antibodies were used for the assay: anti-IP3R1 (rabbit, Santa Cruz, 1/100), anti-GRP75 (rabbit or mouse, Santa Cruz, 1/200), anti-VDAC1 (Mouse, Abcam, Cambridge, UK). Then, cells were incubated with a mixture of MINUS and PLUS secondary PLA probes for 1 h at 37 °C. Duolink anti-rabbit plus probe, anti-mouse minus probe, and anti-goat minus probe were used. All reactions were performed at 37 °C in a humid chamber, with 40 µl of reaction mixture/well. Preparations were mounted in DuoLinkII mounting medium, containing DAPI (Eurogentec). Observations were done with a Zeiss inversed fluorescent microscope, equipped with an ApoTome, using the AxioVision program. Quantification of signals was done with the Duolink Image Tool software or Blobs Finder and expressed as percentage of dots per cytoplasm compared to the non-treated.

2.5. Western blotting

Immunoblotting was performed in mice diaphragm muscles by standard methods using antibodies against: phospho-eIF2α, total eIF2α, GRP78, IRE1, LC3, Beclin-1 (Cell Signaling, Boston, MA); VDAC, RyR, GAPDH (Abcam, Cambridge, UK); IP3R1, ATF6, GRP75 (Santa Cruz Biotechnology, Santa Cruz, CA); MFN2 (Sigma, Saint Louis, USA); Calsequestrin, SERCA1, SERCA2 (Thermo Fisher Scientific, Rockford, USA). Analysis and quantification of proteins (normalized in all cases to GAPDH as loading control) were performed with Image J software version 1.43u (NIH, Bethesda, MD).

2.6. Measurement of skeletal muscle contractile properties

Diaphragm strips and EDL were electrically stimulated to determine intrinsic contractile properties as described previously [38]. After euthanasia, the diaphragm was surgically excised and immediately

transferred to chilled Krebs solution perfused with 95% O_2: 5% CO_2 (pH 7.4). From the central tendon to the rib, a 2 mm wide muscle strip was dissected free and mounted between two electrodes within a jacketed tissue bath chamber filled with continuously perfused Krebs solution warmed to 25 °C. A 4.0 silk thread was used to secure the central tendon to an isometric force transducer. After a 15 min thermoequilibration period, muscle length was gradually adjusted to optimal length (Lo, the length at which maximal twitch force is obtained). The force-frequency relationship was determined by sequential supramaximal stimulation for 1 s over a range of stimulation frequencies (from 10 to 120 Hz) with 2 min between each stimulation train. Fatigue resistance was assessed by measuring the rate of loss of muscle force during repetitive stimulation at 30 Hz over a 10 min period. At the end of the experiment, Lo was directly measured with a microcaliper and the muscle blotted dry and weighed. Specific force (force/cross sectional area) was calculated and expressed in N/cm^2, assuming a muscle density of 1.056 g/cm^3.

2.7. Eccentric contraction

Others strips of diaphragm were used to determine a series of high-stress eccentric (lengthening) contractions. Each contraction involved supramaximal stimulation at 120 Hz for a total of 300 ms; the muscle was held at Lo during the initial 100 ms (isometric component), and then lengthened through a distance of 15% of Lo during the last 200 ms (eccentric component). Peak muscle length was maintained for an additional 100 ms after cessation of the stimulation, followed by a return to Lo during the next 100 ms. A total of four such contractions was imposed on the muscle, each being separated by a 30-s recovery period. Last, a 120-Hz stimulation was performed at Lo to determine the final level of isometric force production after the eccentric contraction protocol. Because the level of damage and dysfunction caused by eccentric contractions is directly correlated with the magnitude of the peak stress imposed on the muscle [15], the isometric force deficit induced by each eccentric contraction was normalized to peak stress as previously described [39].

2.8. Statistical analysis

Data are expressed as means ± SEM. Statistical significance was defined as $p < 0.05$ using Student's unpaired *t*-test or ANOVA (one- or two-way), followed by a Bonferroni selected-comparison test. ANOVA with repeated measured was used concerning calcium and contractile experiments.

3. Results

3.1. ER stress in WT mice is associated with a decreased in SR/ER-mitochondria interactions and a perturbation of Ca^{2+} homeostasis

In order to investigate the impact of UPR on SR/ER-mitochondria interactions in control conditions, we induced an acute ER stress in WT mice by injecting the N-glycosylation inhibitor tunicamycin (TM) [31]. Mice were sacrifed 8 h after a single intraperitoneal injection and the UPR response was confirmed by an increase in GRP78, IRE1α, phospho-eIF2α and total eIF2α protein expression and HSPA5 (GRP78) mRNA level in the diaphragm muscle (Figs. 1A, S1A). However ATF6 gene expression and protein level as well as CHOP gene expression (DdiT3) were not significantly increased (Fig. S1A). In FDB isolated fibers, *in situ* proximity ligation assay revealed a decrease IP3R1-GRP75 and IP3R1-VDAC1 interactions (Fig. 1B–C) whereas IP3R1, GRP75 and VDAC expression levels were not affected (Fig. S3A) indicating a decrease in SR/ER-mitochondria interactions after TM injection.

In FDB fibers isolted from TM-treated mice, field stimulated Ca^{2+} transients showed an increase of the peak at high stimulation frequencies (100, 300 Hz, $p < 0.05$, Fig. 2A-B) but the caffeine-induced SR Ca^{2+} release was not significantly changed (Fig. 2C). Although calsequestrin, mitofusin-2, SERCA2a and RyR1 levels were unchanged, SERCA1 expression was significantly increased in diaphragm muscle after TM injection (Fig. S3B). We next measured mitochondrial Ca^{2+} uptake following a single 100 Hz or 300 Hz tetanus stimulation as previously described (Fig. 2D-E; [34–36]). The rhod-2 signal was significantly decreased in TM-treated mice compared to control (Fig. 2E). Similarly, Ca^{2+} fluxes between mitochondria and SR/ER were monitored upon histamine stimulation, in order to release Ca^{2+} from SR/ER through IP3R (Fig. 2F-H). In WT TM-treated fibers, histamine-induced mitochondrial Ca^{2+} uptake was also reduced (Fig. 2F-H) but the cytosolic Ca^{2+} level under histamine stimulation remained constant (Fig. S2D). Altogether these results demonstrate that TM-induced ER stress leads to decrease the SR/ER-mitochondria interactions and impaired Ca^{2+} movements between the two organelles.

3.2. ER stress impairs muscle contractility and activates cell death pathway

To determine the effects of ER stress on contractile function, we compared the force-generating capacities of untreated (CTL) and treated (TM) mice diaphragm strips and EDL muscles electrically stimulated *ex vivo*. A slight reduction in diaphragm force production was observed but did not reach significance ($p = 0.058$; Fig. 3A) while, the peripheral muscle EDL demonstrated significantly lower force production (− 21%) compared to CTL over a broad range of stimulation frequencies (30 to 120 Hz, $p < 0.05$, Fig. 3B). No change was found concerning fatigue resistance in both muscles (Fig. 3A–B). In parallel, we observed an increase of calpain-1 cleavage (Fig. 3C) after TM injection as well as an increase of autophagy-lysosomal pathway, with increased of Beclin1 and LC3-II protein expression (Fig. 3D).

Altogether these results indicate that TM-induced ER stress altered SR/ER-mitochondria Ca^{2+} transfer, decreased contractile function and increased two major proteolytic systems, the Ca^{2+}-activated calpain and autophagy pathways.

3.3. mdx muscles display an increase in ER stress and a reduction of SR/ER-mitochondria interactions

We next evaluated the ER stress in diaphragm of *mdx* mice. Whatever the age, diaphragm *mdx* mice present an increase in GRP78 protein expression (Fig. 4A). The UPR pathways are differentially activated with the age in *mdx* diaphragm. At early stage (4 to 10 weeks), IRE1α increases (Fig. 4A) whereas at 26 weeks, we only observed an increase in eIF2α phosphorylation (Fig. 4B). Furthermore, at 10 weeks ATF6 expression level was also increased in *mdx* diaphragm muscle (Fig. S1C). In parallel to ER stress markers, we observed a progressive increase in IP3R1 protein expression with age in *mdx* mice (Fig. 4C). Thus, to determine whether SR/ER-mitochondria interactions are affected under ER stress in *mdx* mice, all the subsequent experiments were performed on 10 weeks-old mice where IP3R1 expression as well as GRP75 and VDAC1 were similar between groups despite an increase in ER stress markers (Fig. S3A). At this age, IP3R1-GRP75 and IP3R1-VDAC1 interactions in *mdx* mice compared to WT were significantly decreased (Fig. 4D). In addition, immunoprecipitation of IP3R1 showed a decrease of VDAC1-IP3R1 interaction in diaphragm *mdx* mice compared to WT (Fig. S2A). Moreover, as previously reported [40] *mdx* FDB muscle fibers compared to WT displayed an impaired Ca^{2+} homeostasis with increase in caffeine-induced SR Ca^{2+} release, decreased Ca^{2+} transients amplitude at high frequencies (Fig. S2B-D) and reduced mitochondrial Ca^{2+} uptake compared to WT (Fig. 5F-G). However, at 10 weeks old, expression levels of SERCA1, SERCA2a, calsequestrin, RyR1 and mitofusin 2 were not significantly changed compared to WT diaphragm (Fig. S3B).

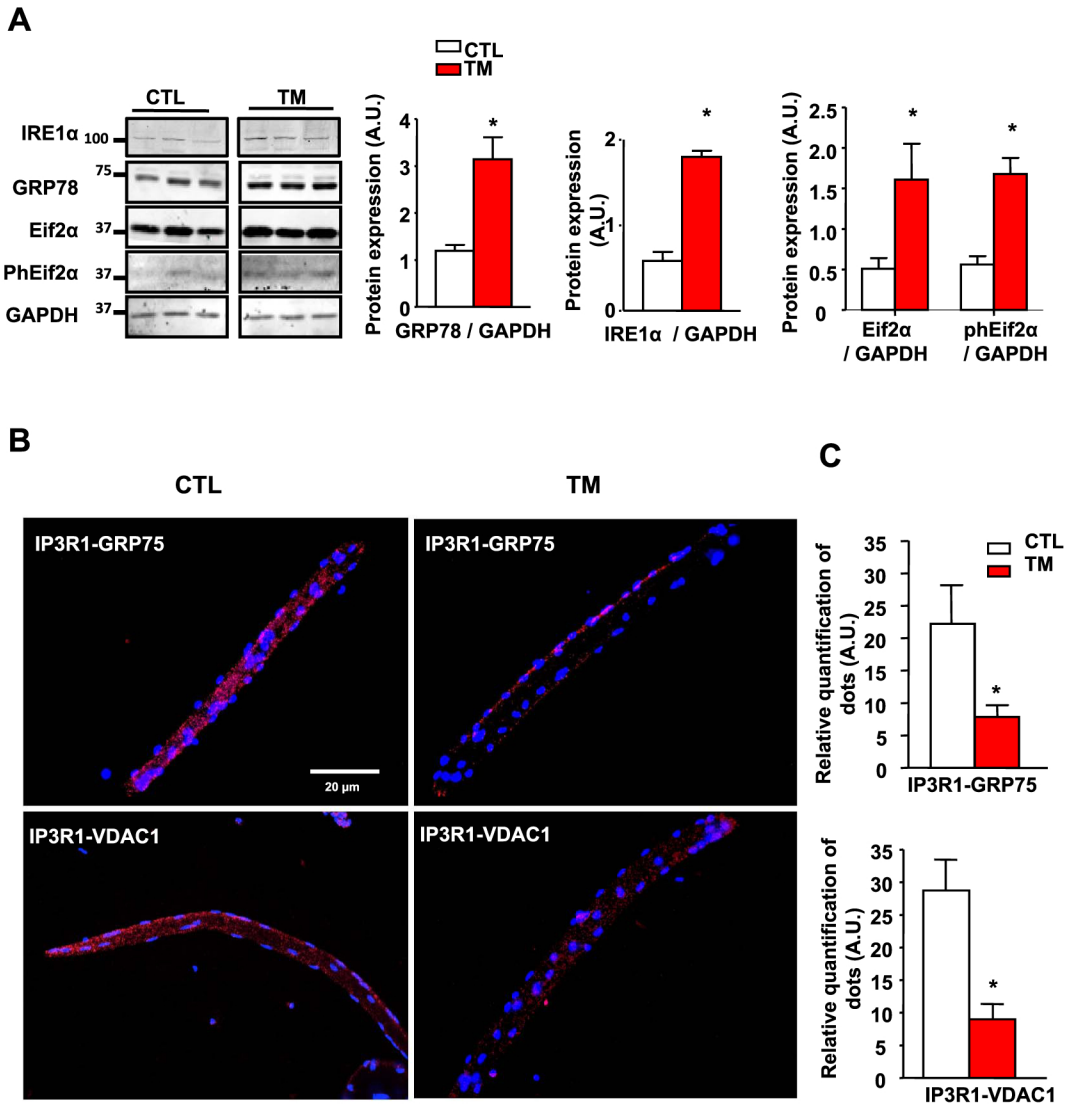

Fig. 1. ER stress induced by tunicamycin (TM) impairs SR/ER-mitochondria interactions in WT muscle. (A) Protein expression of ER stress markers in untreated (CTL) or treated (TM) WT mice diaphragm. Values are means ± SEM, $*p < 0.05$; $n = 3$–6. (B) Representative images of *in situ* PLA on isolated FDB fibers treated (TM, $n = 6$) or not (CTL, $n = 10$–13) with tunycamicin. Nuclei were stained with DAPI and appear in blue. Visualization of protein interaction by *in situ* PLA was evaluated and PLA-specific signals appear in pink dots. Magnification × 20. (C) Using PLA, we evaluated interactions between IP3R1 and GRP75, and IP3R1 and VDAC1 as an intermediate in the Ca^{2+} channeling complex. Values are means ± SEM, $*p < 0.05$ *vs* CTL.

3.4. TUDCA treatment restores SR/ER-mitochondria interactions and improves mdx contractile function

Finally, we assessed the effects of TUDCA, a bile acid derivative, known to reduce ER stress [41]. Chronic TUDCA treatment of *mdx* mice (4 weeks, i.p.) significantly decreased the IRE1α expression compared to untreated *mdx* mice (Fig. 5A-B). At the mRNA level, *Grp78* expression as well as *Atf6* and *DdiT3* are also down-regulated in *mdx* treated with TUDCA (Fig. S2B). In addition, TUDCA treatment restored IP3R1-GRP75 and IP3R1-VDAC interactions (Fig. 5C-D) and improved mitochondrial Ca^{2+} uptake under histamine stimulation as well as after single tetanus stimulation at 100 Hz or 300 Hz (Fig. 5E-G). Further, field-stimulated peak Ca^{2+} transients were also enhanced (Fig. 6A), whereas caffeine-induced SR Ca^{2+} release and histamine-induced SR Ca^{2+} release were non-significantly decreased (Figs. 6B, S2E). In parallel, diaphragmatic contractile specific force was improved after four weeks of TUDCA treatment (Fig. 6C) without any change in fatigue resistance (Fig. 6D). Moreover, for each subsequent eccentric contraction, the loss of force is more dramatic in *mdx* mouse compared to TUDCA treated *mdx* mice (Fig. 6E). Although this contractile function improvement was associated with a decrease of the Ca^{2+} activated calpain-1 (Fig. 6F), SERCA1, SERCA2a, MFN2, calsequestrin and RyR1 expression was unchanged compared to untreated *mdx* diaphragms. Altogether these results demonstrate that decrease ER stress restores SR/ER-mitochondria Ca^{2+} homeostasis and improves contractile function in *mdx* muscle.

4. Discussion

Skeletal muscle which represents 40% of body mass, is an important determinant of metabolic status and global health [42,43]. Skeletal muscles lacking dystrophin present an impaired mitochondrial function, an altered Ca^{2+} handling and muscle dysfunction [16–22]. In the current study, we demonstrate that ER stress associated with dystrophin-deficiency is involved in muscle dysfunction through an altered SR/ER-mitochondria interaction. Moreover, SR/ER-mitochondria interaction, Ca^{2+} homeostasis and muscle contractility were improved by ER stress inhibition in dystrophic muscle.

IP3R is a Ca^{2+} release channel of the ER and has a central role during ER stress (for review [44]) and in many cellular processes

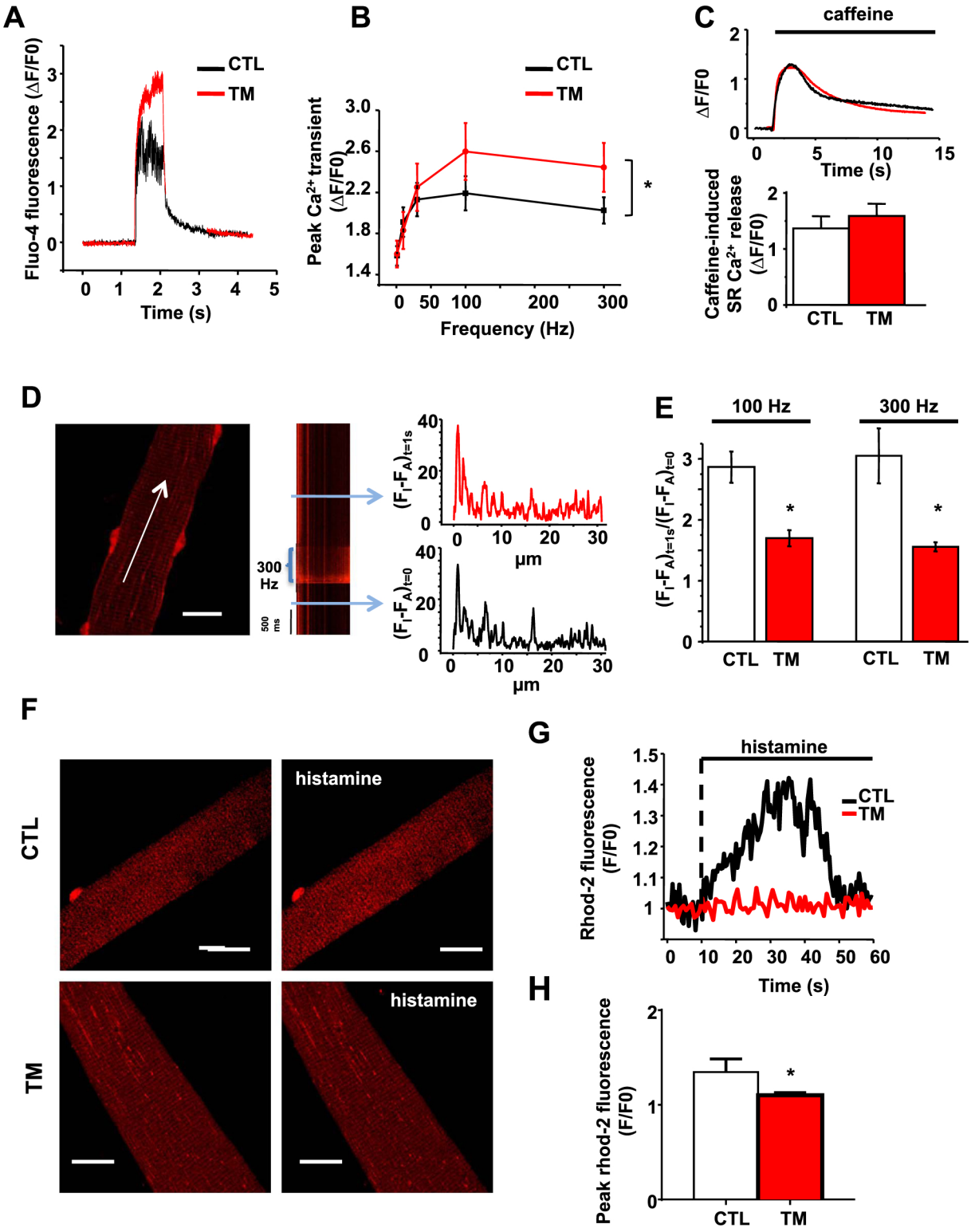

Fig. 2. Tunicamycin induces Ca^{2+} disturbance in WT muscle. (A) Representative Ca^{2+} transients measured by fluo-4 fluorescence during a 100 Hz electrical stimulation. (B) Mean values of peak Ca^{2+} transient at different stimulation rate (1, 10, 30, 100 and 300 Hz) in CTL and TM treated fibers (n = 4–5, fibers = 25–30/group) *$p < 0.05$. (C) Typical example of a caffeine-induced SR Ca^{2+} release recorded in isolated FDB fibers and mean values of the maximal amplitude of caffeine-induced SR Ca^{2+} release in CTL and TM-treated FDB fibers. (D-E) Mitochondrial Ca^{2+} measurement during tetanus stimulation in rhod-2-loaded FDB fibers line-scanned along the long axis of the cell. Rhod-2 signals were first measured 500 ms before (t = 0) and 1 s after (t = 1 s) a 750 ms tetanus stimulation. The rhod-2 signal at t = 1 s is then divided by the rhod-2 signal at t = 0 to calculate F/F0. Mean values ± SEM of F/F0 are then estimated during single tetanus stimulation at 100 Hz or 300 Hz (n = 10–13 FDB fibers per conditions). (F–G) Representative response of mitochondrial Ca^{2+} uptake (rhod-2 fluorescence) after histamine stimulation (100 μmol/l) in CTL (n = 17) and TM (n = 14) treated FDB single fiber. Mean Ca^{2+} flux was normalized to fluorescence values prior to histamine application. Values are means ± SEM, *$p < 0.05$ *vs* TM.

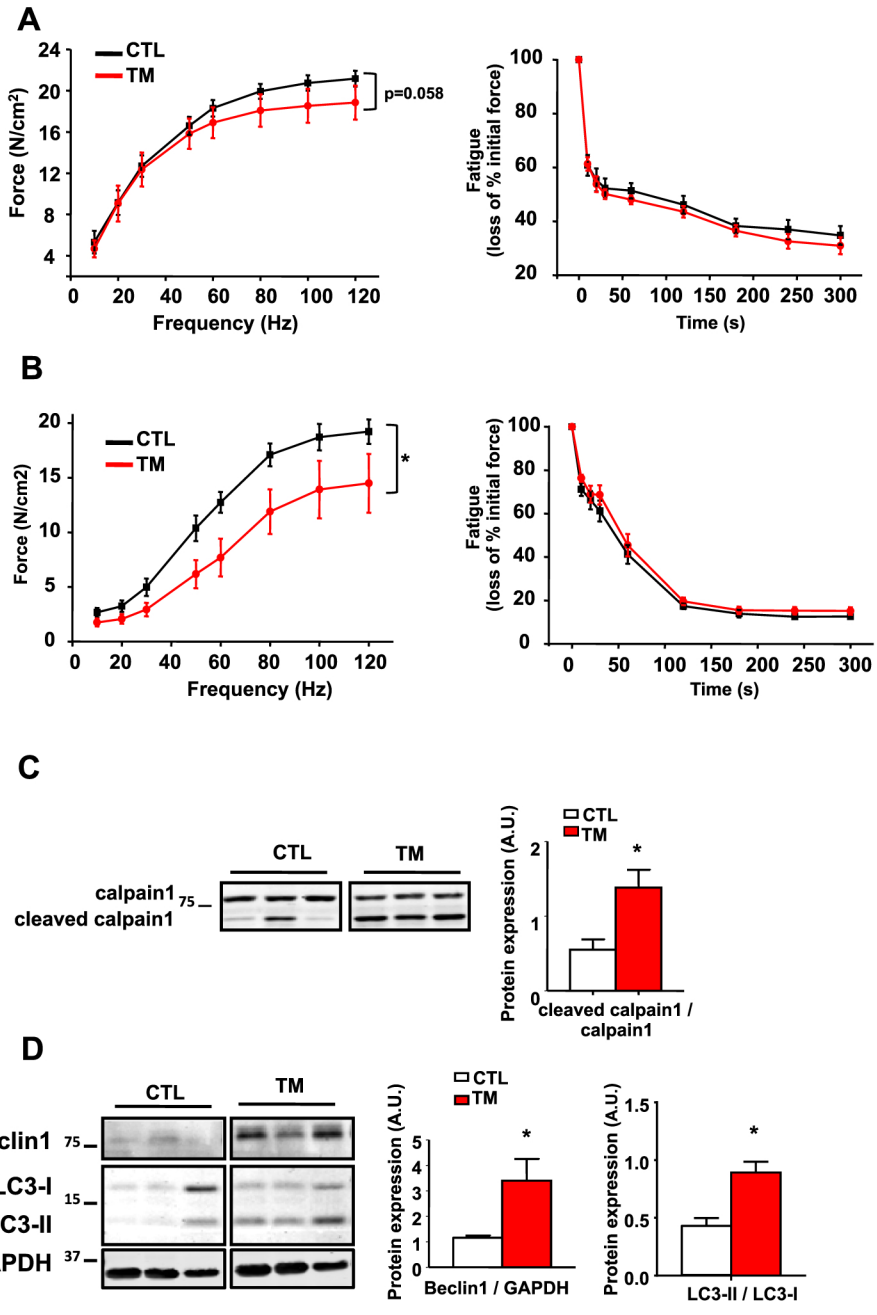

Fig. 3. Tunicamycin induces muscle contractile dysfunction and autophagy pathway in WT muscle mice. Maximal force-generating capacity at different frequencies of electrical stimulation and fatigue resistance during repetitive electrical stimulation of treated (TM) or untreated (CTL) WT diaphragm (A) and EDL (B) *ex vivo*. $^{*}p < 0.05$; $n = 5$-7 per group. Protein expression of calpain-1 (C) and autophagy markers (D) in diaphragm homogenates. Values are means ± SEM, $^{*}p < 0.05$ *vs* TM; $n = 3$–6.

including the regulation of cell fate [45]. SR/ER-mitochondria contact points are known to be enriched in Ca^{2+} handling proteins and chaperones, and to generate microdomains with a high Ca^{2+} concentration. MAMs are regions of the SR/ER tethered to mitochondria and controlling Ca^{2+} transfer between both organelles through the complex formed between the VDAC, GRP75 and IP3R. They participate to cellular metabolism and mitochondrial function [46]. Recently it was demonstrated that ER stress decreases the SR/ER-mitochondria interaction through disruption of MAM integrity and impaired SR/ER-mitochondria Ca^{2+} transfer [8,37].

TM-induced ER stress decreases IP3R-GRP75-VDAC interaction and leads to a disturbed Ca^{2+} equilibrium within the muscle cells. An acute disruption in SR-mitochondria tethering decreases mitochondrial Ca^{2+} uptake capacity which results in an increase in cytosolic Ca^{2+} transients without affecting SR Ca^{2+} load [34,47]. These results demonstrated that the impaired SR-mitochondria interaction, under ER stress, not only impact mitochondrial Ca^{2+} uptake following IP3-induced Ca^{2+} release but also during excitation-contraction coupling, which in turn may affect energy supply. On the other hand, SERCA1 expression was significantly increased suggesting that a decrease in mitochondrial Ca^{2+} uptake might be compensated by an increase SERCA1 to maintain SR Ca^{2+} load. In addition, such disturbance in Ca^{2+} homeostasis leads to activation of proteolytic system such as Ca^{2+}-activated calpain-1 and autophagy processes [17,48]. Here, we showed both an increase in cleaved calpain-1 and autophagy markers. Although autophagy might be considered as a protective adaptive response [49], a prolonged stimulation of autophagy can lead to a so-called autophagic cell death [50]. Moreover, myofilaments degradation upon calpain activation would impaired muscle function [51]. Indeed, muscle contractility experiments reveal a decrease in EDL muscle contractility under ER stress, while the diaphragm seems to be less affected. One limitation of the present study is the duration of the ER stress in WT mice. Indeed, a prolonged ER stress period would have probably induced a more pronounced muscle remodeling and affects more dramatically the

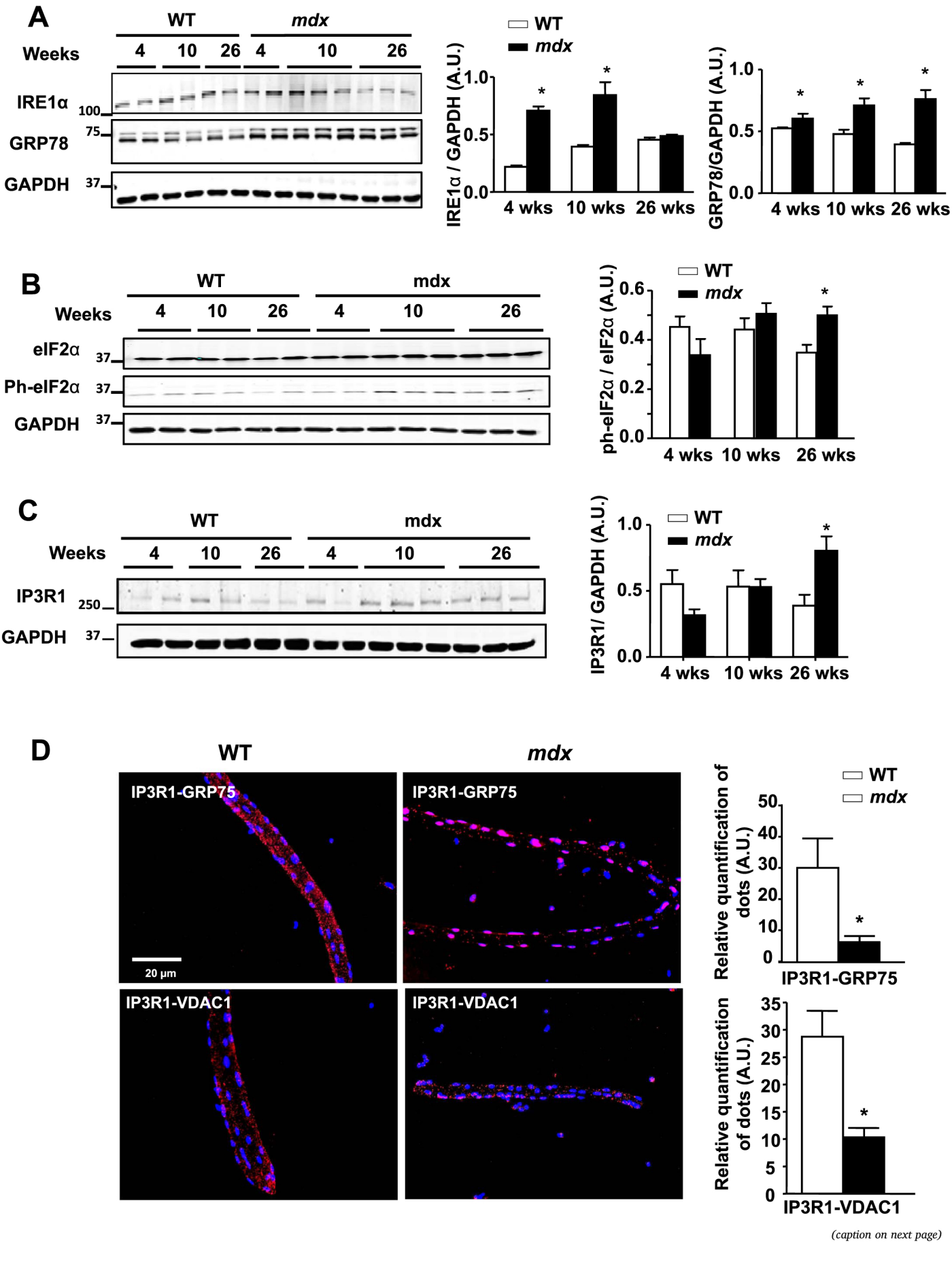

(caption on next page)

Fig. 4. *mdx* diaphragms display an increase of ER stress and an impaired SR/ER-mitochondria interactions. Proteins expressions of ER stress markers in the diaphragm of 4, 10 and 26-weeks old WT and *mdx* mice. Representative immunoblots showing protein expression levels of (A) IRE1α and GRP78; (B) total and phosphorylated forms of eIF2α; (C) IP3R1. Values are means ± SEM, n = 4-6 per group, * $p < 0.05$ WT *vs* mdx. (D) Representative images and quantitative analysis of IPR1-GRP75 and IP3R1-VDAC1 interaction measured by *in situ* PLA on isolated FDB fibers from WT (n = 10-13) or *mdx* (n = 11–17) mice. Nuclei were stained with DAPI and appear in blue. Visualization of protein interaction (PLA-specific signals) appears in pink dots. Magnification: × 20. *$p < 0.05$.

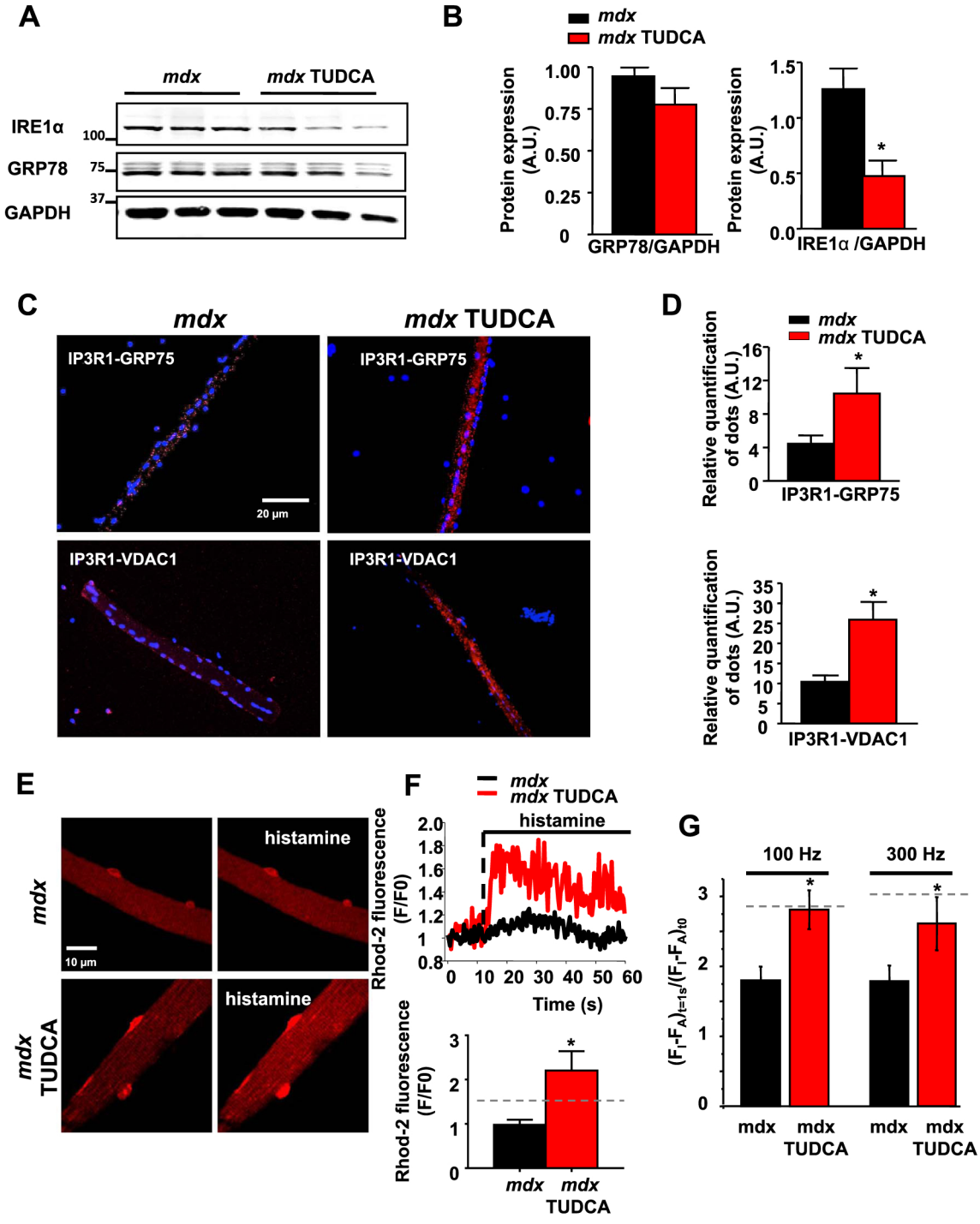

Fig. 5. TUDCA treatment attenuates ER stress and improves SR/ER-mitochondria interactions in *mdx* mice. Proteins expressions of ER stress markers in the diaphragm of untreated (*mdx*) and *mdx*-treated mice (*mdx* TUDCA). Representative immunoblots (A) and graphs (B) showing protein expression levels of GRP78 and IRE1α. All quantifications of proteins are normalized to GAPDH and expressed in arbitrary units. Data are means ± SEM, n = 4–6 per group, * $p < 0.05$ *mdx vs mdx* TUDCA. (C-D) Representative images and quantitative analysis of IP3R1-GRP75 and IP3R1-VDAC1 interaction measured by *in situ* PLA on isolated FDB fibers from *mdx* following, or not, TUDCA treatment. (*E*-F) Representative response and mean values of mitochondrial Ca^{2+}-uptake (rhod-2 fluorescence) after histamine stimulation in FDB single fibers from untreated and TUDCA treated *mdx* mice. Dash lines represent mean value obtained in WT fibers. (G) Mean values of mitochondria Ca^{2+} (rhod-2 fluorescence) after single tetanus stimulation at 100 Hz or 300 Hz. Dash lines represent mean value obtained in WT fibers. Data are expressed as mean ± SEM, n = 4–6 per group, * $p < 0.05$ *mdx vs mdx* TUDCA.

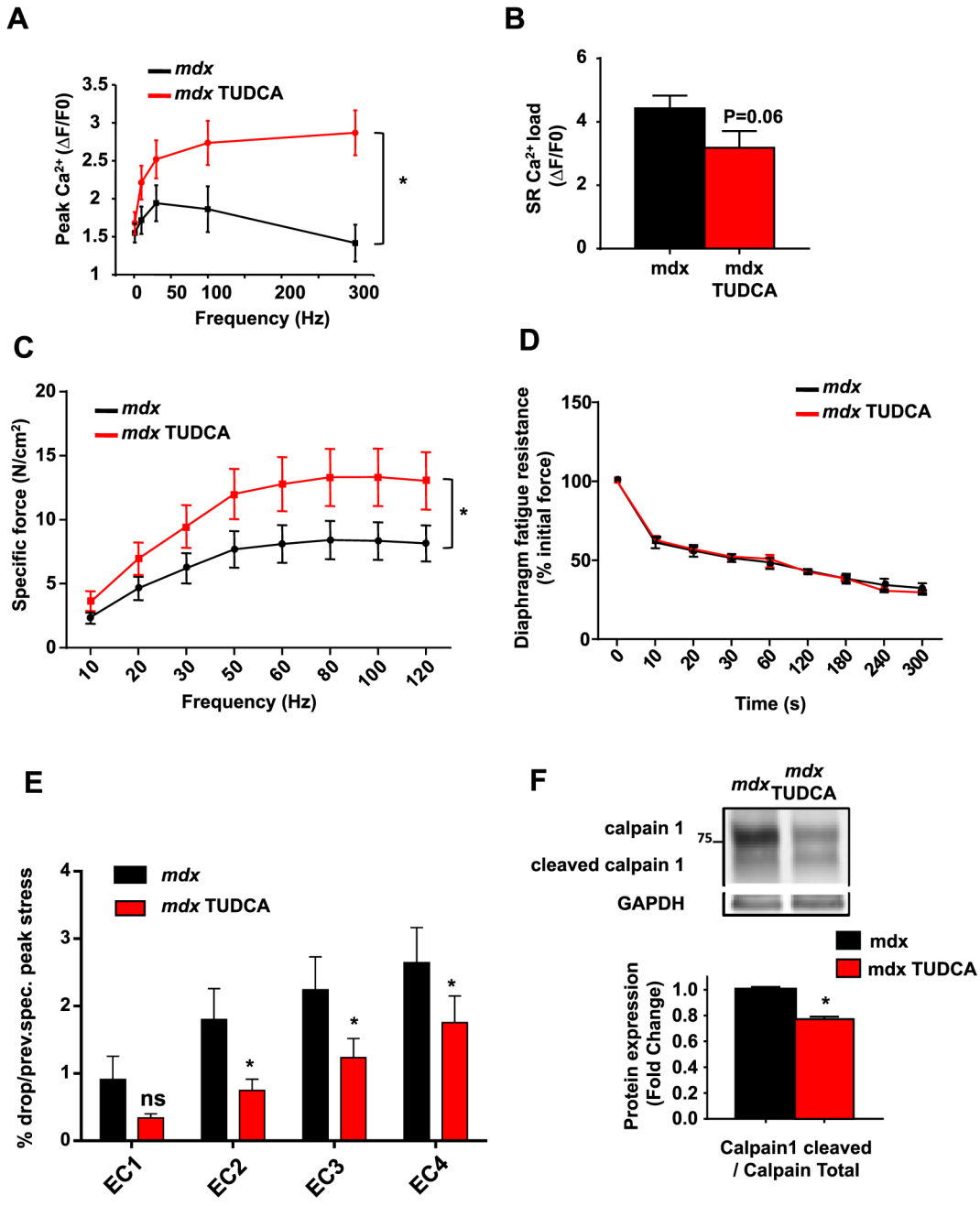

Fig. 6. TUDCA prevents Ca^{2+} disturbance and improves muscle contractility in *mdx* mice. (A) Peak Ca^{2+} transient at different stimulation (1, 10, 30, 100 and 300 Hz) and (B) SR Ca^{2+} load after a caffeine pulse in fibers from untreated and TUDCA treated *mdx* mice. Maximal force-generating capacity at different frequencies of electrical stimulation (C) and fatigue resistance (D) during repetitive electrical stimulation in *ex vivo* diaphragm of *mdx* treated (*mdx* TUDCA) or untreated (*mdx*) mice. (E) Loss of force production after 4 different eccentric contractions (EC) in diaphragm from untreated and TUDCA treated *mdx* mice. Data are expressed as mean ± SEM: $n = 5–7$; $^*p < 0.05$. (F) Protein expression of cleaved calpain 1 in diaphragm of untreated and treated *mdx* mice. Values are means ± SEM; $n = 3–6$. $^*p < 0.05$.

diaphragm function as seen in the *mdx* model.

Indeed, ER stress was reported in DMD patients highlighting the hypothesis of ER stress in this pathology. Here, we confirm that the UPR is activated and we demonstrate a SR/ER-mitochondria-Ca^{2+} disturbance in dystrophic muscle. In *mdx* diaphragm, UPR markers such as GRP78, IRE1, phospho-eIF2α increase at the age of 4 weeks up to 10 weeks. Then, with aging, an alternative activation of two different pathways of UPR (PERK and IRE1α) occurs. Our data are consistent with previous data demonstrating that the ER chaperone GRP78 was increased in DMD patients compared to healthy individuals [13]. In our study, ER stress-related to age is associated with an increase of IP3R1 expression in *mdx* mice diaphragm, while WT muscle mice evolve in the opposite way. This could be interpreted as a system to compensate the SR/ER-mitochondria interaction disruption [52]. The exact mechanisms leading to ER stress in *mdx* mice are unclear but might involve, at least partly, Ca^{2+} handling perturbation [2]. Indeed, ER stress and Ca^{2+} homeostasis are closely inter-connected, with an impaired ER-mitochondria Ca^{2+} transfer and increase in ER Ca^{2+} store [8]. Here, the decrease SR/ER-mitochondrial Ca^{2+} transfer was also accompanied by an increase in caffeine-induced SR Ca^{2+} release, which might be interpreted as an increase in SR Ca^{2+} load. Several studies have reported an altered SR function in mdx skeletal fibers characterized by an altered SR Ca^{2+} release [53] and RyR dysfunction [17,54,55] and a remodeling in SERCA activity [56–60] with an elevation of resting Ca^{2+} concentration in skeletal muscles of *mdx* mice. In addition, depending on the muscle fiber type, the stage of the pathology and the

protocol used to measure SR Ca^{2+} content, the SR Ca^{2+} load has been reported by several groups to be either decreased, unchanged or increased [61–64]. A modification in RyR1 sensitivity to caffeine might account at least partly to the increase in the caffeine-induced SR Ca^{2+} release in *mdx* mice.

Finally, we treated *mdx* mice with TUDCA, an ER chaperone tauroursodeoxycholic acid widely used to suppress ER stress [65,66]. This treatment reduced IRE1α expression, *Atf6*, *Ddit3* and *Grp78* gene expression indicating a decreased in both UPR response pathways in *mdx* skeletal muscle. In addition, SR/ER mitochondria interaction and Ca^{2+} transfer were restored and concomitantly, Ca^{2+} transients increased and contractile function improved. Surprisingly, TUDCA treatment did not change the expression levels of the main proteins involved in Ca^{2+} handling but improved important aspects of contractile function in *mdx* muscle: diaphragmatic muscle force and resistance to eccentric contraction-induced force lost. Similarly, Carlson et al. have shown that another ursodeoxycholic acid (UDCA) has beneficial effects on the structure and function of *mdx* muscle [67]. Although they did not explore ER stress pathways and SR-mitochondria Ca^{2+} transfer, they attributed these benefits to the inhibition of inflammatory pathway mediated by NF-kB activation. Eccentric damage and loss of muscle force are important causes of muscle weakness in skeletal muscle of *mdx* mice and DMD patients. Although the mitochondrial (dys)function was not specifically assessed in the present study, increase SR/ER-mitochondria interaction might improve mitochondrial function in DMD and ATP supply favoring both an increase in Ca^{2+} transients and contractile function. In addition, TUDCA treatment decrease calpain-1 cleavage which is in line with the proposed model whereby UPR activates proteolytic pathway and impaired muscle function in the *mdx* mice [13].

To conclude, the present work revealed several new findings and brings original data on ER stress regulation to maintain efficient SR/ER-mitochondria interaction, associated with adaptive Ca^{2+} flux and normal muscular function. Although an acute pharmacological induction of ER stress in WT mice does not reproduces the DMD phenotype, improvement of SR/ER–mitochondria Ca^{2+} transfer under TUDCA treatment highlighted the complexity and sensibility of the stress response in healthy and dystrophic tissue and revealed the therapeutical potential to modulate this pathway in muscular pathology.

Author contributions

M.P., A.L., S.M., J.F designed the study, performed and analyzed the experiments and write the manuscript; C. AP. performed and analyzed biochemical experiments; H.D. contributed to the contractile function, C.N. and V. S. performed supplemental experiments.

Conflict of interest

The authors declare no competing financial interests.

Acknowledgements

A.L. and J.F. were supported by the Fondation de France (No. 00056858), AFM (15083 and 15862), and FRM (R133063FC).

References

[1] M.J. Berridge, The endoplasmic reticulum: a multifunctional signaling organelle, Cell Calcium 32 (2002) 235–249.

[2] J. Krebs, The plethora of PMCA isoforms: alternative splicing and differential expression, Biochim. Biophys. Acta 1853 (2015) 2018–2024, http://dx.doi.org/10.1016/j.bbamcr.2014.12.020.

[3] K. Zhang, R.J. Kaufman, Protein folding in the endoplasmic reticulum and the unfolded protein response, Handb. Exp. Pharmacol. (2006) 69–91.

[4] H. Malhi, R.J. Kaufman, Endoplasmic reticulum stress in liver disease, J. Hepatol. 54 (2011) 795–809, http://dx.doi.org/10.1016/j.jhep.2010.11.005.

[5] E. Szegezdi, S.E. Logue, A.M. Gorman, A. Samali, Mediators of endoplasmic reticulum stress-induced apoptosis, EMBO Rep. 7 (2006) 880–885, http://dx.doi.org/10.1038/sj.embor.7400779.

[6] C. Giorgi, D. De Stefani, A. Bononi, R. Rizzuto, P. Pinton, Structural and functional link between the mitochondrial network and the endoplasmic reticulum, Int. J. Biochem. Cell Biol. 41 (2009) 1817–1827, http://dx.doi.org/10.1016/j.biocel.2009.04.010.

[7] G. Szabadkai, K. Bianchi, P. Várnai, D. De Stefani, M.R. Wieckowski, D. Cavagna, A.I. Nagy, T. Balla, R. Rizzuto, Chaperone-mediated coupling of endoplasmic reticulum and mitochondrial Ca2 + channels, J. Cell Biol. 175 (2006) 901–911, http://dx.doi.org/10.1083/jcb.200608073.

[8] J. Rieusset, J. Fauconnier, M. Paillard, E. Belaidi, E. Tubbs, M.-A. Chauvin, A. Durand, A. Bravard, G. Teixeira, B. Bartosch, M. Michelet, P. Theurey, G. Vial, M. Demion, E. Blond, F. Zoulim, L. Gomez, H. Vidal, A. Lacampagne, M. Ovize, Disruption of calcium transfer from ER to mitochondria links alterations of mitochondria-associated ER membrane integrity to hepatic insulin resistance, Diabetologia 59 (2016) 614–623, http://dx.doi.org/10.1007/s00125-015-3829-8.

[9] Z. Yu, A.M. Wang, H. Adachi, M. Katsuno, G. Sobue, Z. Yue, D.M. Robins, A.P. Lieberman, Macroautophagy is regulated by the UPR-mediator CHOP and accentuates the phenotype of SBMA mice, PLoS Genet. 7 (2011) e1002321, , http://dx.doi.org/10.1371/journal.pgen.1002321.

[10] K. Ikezoe, M. Nakamori, H. Furuya, H. Arahata, S. Kanemoto, T. Kimura, K. Imaizumi, M.P. Takahashi, S. Sakoda, N. Fujii, J. Kira, Endoplasmic reticulum stress in myotonic dystrophy type 1 muscle, Acta Neuropathol. (Berl.) 114 (2007) 527–535, http://dx.doi.org/10.1007/s00401-007-0267-9.

[11] M. Vitadello, A. Doria, E. Tarricone, A. Ghirardello, L. Gorza, Myofiber stress-response in myositis: parallel investigations on patients and experimental animal models of muscle regeneration and systemic inflammation, Arthritis Res. Ther. 12 (2010) R52, http://dx.doi.org/10.1186/ar2963.

[12] M. Screen, O. Raheem, J. Holmlund-Hampf, P.H. Jonson, S. Huovinen, P. Hackman, B. Udd, Gene expression profiling in tibial muscular dystrophy reveals unfolded protein response and altered autophagy, PLoS One 9 (2014) e90819, , http://dx.doi.org/10.1371/journal.pone.0090819.

[13] C. Moorwood, E.R. Barton, Caspase-12 ablation preserves muscle function in the mdx mouse, Hum. Mol. Genet. (2014), http://dx.doi.org/10.1093/hmg/ddu249.

[14] E.P. Hoffman, R.H. Brown, L.M. Kunkel, Dystrophin: the protein product of the Duchenne muscular dystrophy locus, Cell 51 (1987) 919–928.

[15] B.J. Petrof, J.B. Shrager, H.H. Stedman, A.M. Kelly, H.L. Sweeney, Dystrophin protects the sarcolemma from stresses developed during muscle contraction, Proc. Natl. Acad. Sci. U. S. A. 90 (1993) 3710–3714.

[16] A.J. Bakker, S.I. Head, D.A. Williams, D.G. Stephenson, Ca2 + levels in myotubes grown from the skeletal muscle of dystrophic (mdx) and normal mice, J. Physiol. 460 (1993) 1–13.

[17] A.M. Bellinger, S. Reiken, C. Carlson, M. Mongillo, X. Liu, L. Rothman, S. Matecki, A. Lacampagne, A.R. Marks, Hypernitrosylated ryanodine receptor calcium release channels are leaky in dystrophic muscle, Nat. Med. 15 (2009) 325–330, http://dx.doi.org/10.1038/nm.1916.

[18] B. Constantin, S. Sebille, C. Cognard, New insights in the regulation of calcium transfers by muscle dystrophin-based cytoskeleton: implications in DMD, J. Muscle Res. Cell Motil. 27 (2006) 375–386, http://dx.doi.org/10.1007/s10974-006-9085-2.

[19] J. Fauconnier, J. Thireau, S. Reiken, C. Cassan, S. Richard, S. Matecki, A.R. Marks, A. Lacampagne, Leaky RyR2 trigger ventricular arrhythmias in Duchenne muscular dystrophy, Proc. Natl. Acad. Sci. U. S. A. 107 (2010) 1559–1564, http://dx.doi.org/10.1073/pnas.0908540107.

[20] P.Y. Fong, P.R. Turner, W.F. Denetclaw, R.A. Steinhardt, Increased activity of calcium leak channels in myotubes of Duchenne human and mdx mouse origin, Science 250 (1990) 673–676.

[21] N. Imbert, C. Cognard, G. Duport, C. Guillou, G. Raymond, Abnormal calcium homeostasis in Duchenne muscular dystrophy myotubes contracting in vitro, Cell Calcium 18 (1995) 177–186.

[22] P.R. Turner, P.Y. Fong, W.F. Denetclaw, R.A. Steinhardt, Increased calcium influx in dystrophic muscle, J. Cell Biol. 115 (1991) 1701–1712.

[23] A.V. Kuznetsov, K. Winkler, F.R. Wiedemann, P. von Bossanyi, K. Dietzmann, W.S. Kunz, Impaired mitochondrial oxidative phosphorylation in skeletal muscle of the dystrophin-deficient mdx mouse, Mol. Cell. Biochem. 183 (1998) 87–96.

[24] M. Pauly, F. Daussin, Y. Burelle, T. Li, R. Godin, J. Fauconnier, C. Koechlin-Ramonatxo, G. Hugon, A. Lacampagne, M. Coisy-Quivy, F. Liang, S. Hussain, S. Matecki, B.J. Petrof, AMPK activation stimulates autophagy and ameliorates muscular dystrophy in the mdx mouse diaphragm, Am. J. Pathol. 181 (2012) 583–592, http://dx.doi.org/10.1016/j.ajpath.2012.04.004.

[25] G.L. Warren, D.A. Hayes, D.A. Lowe, R.B. Armstrong, Mechanical factors in the initiation of eccentric contraction-induced injury in rat soleus muscle, J. Physiol. 464 (1993) 457–475.

[26] J.M. Gillis, Understanding dystrophinopathies: an inventory of the structural and functional consequences of the absence of dystrophin in muscles of the mdx mouse, J. Muscle Res. Cell Motil. 20 (1999) 605–625.

[27] M. Sandri, U. Carraro, M. Podhorska-Okolov, C. Rizzi, P. Arslan, D. Monti, C. Franceschi, Apoptosis, DNA damage and ubiquitin expression in normal and mdx muscle fibers after exercise, FEBS Lett. 373 (1995) 291–295.

[28] J.G. Tidball, D.E. Albrecht, B.E. Lokensgard, M.J. Spencer, Apoptosis precedes necrosis of dystrophin-deficient muscle, J. Cell Sci. 108 (Pt 6) (1995) 2197–2204.

[29] M. Galán, M. Kassan, S.-K. Choi, M. Partyka, M. Trebak, D. Henrion, K. Matrougui, A novel role for epidermal growth factor receptor tyrosine kinase and its downstream endoplasmic reticulum stress in cardiac damage and microvascular dysfunction in type 1 diabetes mellitus, Hypertension 60 (2012) 71–80, http://dx.doi.org/10.1161/HYPERTENSIONAHA.112.192500.

[30] J. Wu, D.T. Rutkowski, M. Dubois, J. Swathirajan, T. Saunders, J. Wang, B. Song, G.D.-Y. Yau, R.J. Kaufman, ATF6alpha optimizes long-term endoplasmic reticulum function to protect cells from chronic stress, Dev. Cell 13 (2007) 351–364, http://dx.doi.org/10.1016/j.devcel.2007.07.005.

[31] D.T. Rutkowski, J. Wu, S.-H. Back, M.U. Callaghan, S.P. Ferris, J. Iqbal, R. Clark, H. Miao, J.R. Hassler, J. Fornek, M.G. Katze, M.M. Hussain, B. Song, J. Swathirajan, J. Wang, G.D.-Y. Yau, R.J. Kaufman, UPR pathways combine to prevent hepatic steatosis caused by ER stress-mediated suppression of transcriptional master regulators, Dev. Cell 15 (2008) 829–840, http://dx.doi.org/10.1016/j.devcel.2008.10.015.

[32] S.I. Head, Membrane potential, resting calcium and calcium transients in isolated muscle fibres from normal and dystrophic mice, J. Physiol. 469 (1993) 11–19.

[33] A. Takahashi, P. Camacho, J.D. Lechleiter, B. Herman, Measurement of intracellular calcium, Physiol. Rev. 79 (1999) 1089–1125.

[34] A. Ainbinder, S. Boncompagni, F. Protasi, R.T. Dirksen, Role of Mitofusin-2 in mitochondrial localization and calcium uptake in skeletal muscle, Cell Calcium 57 (2015) 14–24, http://dx.doi.org/10.1016/j.ceca.2014.11.002.

[35] A.E. Rossi, S. Boncompagni, L. Wei, F. Protasi, R.T. Dirksen, Differential impact of mitochondrial positioning on mitochondrial Ca(2 +) uptake and Ca(2 +) spark suppression in skeletal muscle, Am. J. Physiol. Cell Physiol. 301 (2011) C1128–C1139, http://dx.doi.org/10.1152/ajpcell.00194.2011.

[36] J. Bruton, P. Tavi, J. Aydin, H. Westerblad, J. Lännergren, Mitochondrial and myoplasmic [Ca2 +] in single fibres from mouse limb muscles during repeated tetanic contractions, J. Physiol. 551 (2003) 179–190, http://dx.doi.org/10.1113/jphysiol.2003.043927.

[37] M. Paillard, E. Tubbs, P.-A. Thiebaut, L. Gomez, J. Fauconnier, C.C. Da Silva, G. Teixeira, N. Mewton, E. Belaidi, A. Durand, M. Abrial, A. Lacampagne, J. Rieusset, M. Ovize, Depressing mitochondria-reticulum interactions protects cardiomyocytes from lethal hypoxia-reoxygenation injury, Circulation 128 (2013) 1555–1565, http://dx.doi.org/10.1161/CIRCULATIONAHA.113.001225.

[38] S. Matecki, G.H. Guibinga, B.J. Petrof, Regenerative capacity of the dystrophic (mdx) diaphragm after induced injury, Am. J. Physiol. Regul. Integr. Comp. Physiol. 287 (2004) R961–R968, http://dx.doi.org/10.1152/ajpregu.00146.2004.

[39] R. Gilbert, R.W.R. Dudley, A.-B. Liu, B.J. Petrof, J. Nalbantoglu, G. Karpati, Prolonged dystrophin expression and functional correction of mdx mouse muscle following gene transfer with a helper-dependent (gutted) adenovirus-encoding murine dystrophin, Hum. Mol. Genet. 12 (2003) 1287–1299, http://dx.doi.org/10.1093/hmg/ddg141.

[40] D.G. Allen, O.L. Gervasio, E.W. Yeung, N.P. Whitehead, Calcium and the damage pathways in muscular dystrophy, Can. J. Physiol. Pharmacol. 88 (2010) 83–91, http://dx.doi.org/10.1139/y09-058.

[41] U. Ozcan, Q. Cao, E. Yilmaz, A.-H. Lee, N.N. Iwakoshi, E. Ozdelen, G. Tuncman, C. Görgün, L.H. Glimcher, G.S. Hotamisligil, Endoplasmic reticulum stress links obesity, insulin action, and type 2 diabetes, Science 306 (2004) 457–461, http://dx.doi.org/10.1126/science.1103160.

[42] W.R. Frontera, J. Ochala, Skeletal muscle: a brief review of structure and function, Calcif. Tissue Int. 96 (2015) 183–195, http://dx.doi.org/10.1007/s00223-014-9915-y.

[43] W.R. Frontera, V.A. Hughes, K.J. Lutz, W.J. Evans, A cross-sectional study of muscle strength and mass in 45- to 78-yr-old men and women, J. Appl. Physiol. Bethesda Md. 1985 71 (1991) 644–650.

[44] S. Kiviluoto, T. Vervliet, H. Ivanova, J.-P. Decuypere, H. De Smedt, L. Missiaen, G. Bultynck, J.B. Parys, Regulation of inositol 1,4,5-trisphosphate receptors during endoplasmic reticulum stress, Biochim. Biophys. Acta 1833 (2013) 1612–1624, http://dx.doi.org/10.1016/j.bbamcr.2013.01.026.

[45] M.J. Berridge, P. Lipp, M.D. Bootman, The versatility and universality of calcium signalling, Nat. Rev. Mol. Cell Biol. 1 (2000) 11–21, http://dx.doi.org/10.1038/35036035.

[46] C. Cárdenas, R.A. Miller, I. Smith, T. Bui, J. Molgó, M. Müller, H. Vais, K.-H. Cheung, J. Yang, I. Parker, C.B. Thompson, M.J. Birnbaum, K.R. Hallows, J.K. Foskett, Essential regulation of cell bioenergetics by constitutive InsP3 receptor Ca2 + transfer to mitochondria, Cell 142 (2010) 270–283, http://dx.doi.org/10.1016/j.cell.2010.06.007.

[47] C. Maack, B. O'Rourke, Excitation-contraction coupling and mitochondrial energetics, Basic Res. Cardiol. 102 (2007) 369–392, http://dx.doi.org/10.1007/s00395-007-0666-z.

[48] M. Sandri, Protein breakdown in muscle wasting: role of autophagy-lysosome and ubiquitin-proteasome, Int. J. Biochem. Cell Biol. (2013), http://dx.doi.org/10.1016/j.biocel.2013.04.023.

[49] I. Azuelos, B. Jung, M. Picard, F. Liang, T. Li, C. Lemaire, C. Giordano, S. Hussain, B.J. Petrof, Relationship between autophagy and ventilator-induced diaphragmatic dysfunction, Anesthesiology 122 (2015) 1349–1361, http://dx.doi.org/10.1097/ALN.0000000000000656.

[50] G. Kroemer, B. Levine, Autophagic cell death: the story of a misnomer, Nat. Rev. Mol. Cell Biol. 9 (2008) 1004–1010, http://dx.doi.org/10.1038/nrm2529.

[51] J. Wu, R.J. Kaufman, From acute ER stress to physiological roles of the unfolded protein response, Cell Death Differ. 13 (2006) 374–384, http://dx.doi.org/10.1038/sj.cdd.4401840.

[52] J.-P. Decuypere, G. Monaco, L. Missiaen, H. De Smedt, J.B. Parys, G. Bultynck, IP(3) receptors, mitochondria, and ca signaling: implications for aging, J. Aging Res. 2011 (2011) 920178, http://dx.doi.org/10.4061/2011/920178.

[53] J. Capote, M. DiFranco, J.L. Vergara, Excitation-contraction coupling alterations in mdx and utrophin/dystrophin double knockout mice: a comparative study, Am. J. Physiol. Cell Physiol. 298 (2010) C1077–C1086, http://dx.doi.org/10.1152/ajpcell.00428.2009.

[54] J.M. Alderton, R.A. Steinhardt, Calcium influx through calcium leak channels is responsible for the elevated levels of calcium-dependent proteolysis in dystrophic myotubes, J. Biol. Chem. 275 (2000) 9452–9460.

[55] G. Robin, C. Berthier, B. Allard, Sarcoplasmic reticulum Ca2 + permeation explored from the lumen side in mdx muscle fibers under voltage control, J. Gen. Physiol. 139 (2012) 209–218, http://dx.doi.org/10.1085/jgp.201110738.

[56] M.E. Kargacin, G.J. Kargacin, The sarcoplasmic reticulum calcium pump is functionally altered in dystrophic muscle, Biochim. Biophys. Acta 1290 (1996) 4–8.

[57] A. Divet, A.-M. Lompré, C. Huchet-Cadiou, Effect of cyclopiazonic acid, an inhibitor of the sarcoplasmic reticulum Ca-ATPase, on skeletal muscles from normal and mdx mice, Acta Physiol. Scand. 184 (2005) 173–186, http://dx.doi.org/10.1111/j.1365-201X.2005.01450.x.

[58] A. Divet, C. Huchet-Cadiou, Sarcoplasmic reticulum function in slow- and fast-twitch skeletal muscles from mdx mice, Pflugers Arch. 444 (2002) 634–643, http://dx.doi.org/10.1007/s00424-002-0854-5.

[59] S.M. Gehrig, R. Koopman, T. Naim, C. Tjoakarfa, G.S. Lynch, Making fast-twitch dystrophic muscles bigger protects them from contraction injury and attenuates the dystrophic pathology, Am. J. Pathol. 176 (2010) 29–33, http://dx.doi.org/10.2353/ajpath.2010.090760.

[60] S.M. Gehrig, C. van der Poel, T.A. Sayer, J.D. Schertzer, D.C. Henstridge, J.E. Church, S. Lamon, A.P. Russell, K.E. Davies, M.A. Febbraio, G.S. Lynch, Hsp72 preserves muscle function and slows progression of severe muscular dystrophy, Nature 484 (2012) 394–398, http://dx.doi.org/10.1038/nature10980.

[61] J.S. Schneider, M. Shanmugam, J.P. Gonzalez, H. Lopez, R. Gordan, D. Fraidenraich, G.J. Babu, Increased sarcolipin expression and decreased sarco (endo)plasmic reticulum Ca2 + uptake in skeletal muscles of mouse models of Duchenne muscular dystrophy, J. Muscle Res. Cell Motil. 34 (2013) 349–356, http://dx.doi.org/10.1007/s10974-013-9350-0.

[62] A. Takagi, S. Kojima, M. Ida, M. Araki, Increased leakage of calcium ion from the sarcoplasmic reticulum of the mdx mouse, J. Neurol. Sci. 110 (1992) 160–164.

[63] X. Zhao, J.G. Moloughney, S. Zhang, S. Komazaki, N. Weisleder, Orai1 mediates exacerbated Ca(2 +) entry in dystrophic skeletal muscle, PLoS One 7 (2012) e49862, , http://dx.doi.org/10.1371/journal.pone.0049862.

[64] V. Robert, M.L. Massimino, V. Tosello, R. Marsault, M. Cantini, V. Sorrentino, T. Pozzan, Alteration in calcium handling at the subcellular level in mdx myotubes, J. Biol. Chem. 276 (2001) 4647–4651, http://dx.doi.org/10.1074/jbc.M006337200.

[65] J. Rieusset, Contribution of mitochondria and endoplasmic reticulum dysfunction in insulin resistance: distinct or interrelated roles? Diabete Metab. 41 (2015) 358–368, http://dx.doi.org/10.1016/j.diabet.2015.02.006.

[66] S. Turdi, N. Hu, J. Ren, Tauroursodeoxycholic acid mitigates high fat diet-induced cardiomyocyte contractile and intracellular Ca2 + anomalies, PLoS One 8 (2013) e63615, , http://dx.doi.org/10.1371/journal.pone.0063615.

[67] C.G. Carlson, R. Potter, V. Yu, K. Luo, J. Lavin, C. Nielsen, In vivo treatment with the NF-κB inhibitor ursodeoxycholic acid (UDCA) improves tension development in the isolated mdx costal diaphragm, Muscle Nerve 53 (2016) 431–437, http://dx.doi.org/10.1002/mus.24755.